INTERNATIONAL JOURNAL OF
RADIATION ONCOLOGY • BIOLOGY • PHYSICS
www.redjournal.org

PHYSICS CONTRIBUTION

FLASH Effects Induced by Orthovoltage X-Rays

Devin Miles, PhD,[a] Daniel Sforza, PhD,[a] John W. Wong, PhD,[a] Kathleen Gabrielson, DVM, PhD,[b] Khaled Aziz, MD, PhD,[a] Mahadevappa Mahesh, MS, PhD,[c] Jonathan B. Coulter, PhD,[d] Ismaeel Siddiqui, BA,[a] Phuoc T. Tran, MD, PhD,[a,e] Akila N. Viswanathan, MD, MPH, MSc,[a] and Mohammad Rezaee, PhD[a]

[a]*Department of Radiation Oncology and Molecular Radiation Sciences, Johns Hopkins University School of Medicine, Baltimore, Maryland;* [b]*Department of Molecular and Comparative Pathobiology, Johns Hopkins University School of Medicine, Baltimore, Maryland;* [c]*Department of Radiology and Radiological Science, Johns Hopkins University School of Medicine, Baltimore, Maryland;* [d]*Department of Urology, Johns Hopkins University School of Medicine, Baltimore, Maryland; and* [e]*Department of Radiation Oncology, University of Maryland School of Medicine, Baltimore, Maryland*

Received Mar 21, 2023; Accepted for publication Jun 11, 2023

Purpose: This work describes the first implementation and in vivo study of ultrahigh-dose-rate radiation (>37 Gy/s; FLASH) effects induced by kilovoltage (kV) x-ray from a rotating-anode x-ray source.

Methods and Materials: A high-capacity rotating-anode x-ray tube with an 80-kW generator was implemented for preclinical FLASH radiation research. A custom 3-dimensionally printed immobilization and positioning tool was developed for reproducible irradiation of a mouse hind limb. Calibrated Gafchromic (EBT3) film and thermoluminescent dosimeters (LiF:Mg,Ti) were used for in-phantom and in vivo dosimetry. Healthy FVB/N and FVBN/C57BL/6 outbred mice were irradiated on 1 hind leg to doses up to 43 Gy at FLASH (87 Gy/s) and conventional (CONV; <0.05 Gy/s) dose rates. The radiation doses were delivered using a single pulse with the widths up to 500 ms and 15 minutes at FLASH and CONV dose rates. Histologic assessment of radiation-induced skin damage was performed at 8 weeks posttreatment. Tumor growth suppression was assessed using a B16F10 flank tumor model in C57BL6J mice irradiated to 35 Gy at both FLASH and CONV dose rates.

Results: FLASH-irradiated mice experienced milder radiation-induced skin injuries than CONV-irradiated mice, visible by 4 weeks posttreatment. At 8 weeks posttreatment, normal tissue injury was significantly reduced in FLASH-irradiated animals compared with CONV-irradiated animals for histologic endpoints including inflammation, ulceration, hyperplasia, and fibrosis. No difference in tumor growth response was observed between FLASH and CONV irradiations at 35 Gy. The normal tissue sparing effects of FLASH irradiations were observed only for high-severity endpoint of ulceration at 43 Gy, which suggests the dependency of biologic endpoints to FLASH radiation dose.

Conclusions: Rotating-anode x-ray sources can achieve FLASH dose rates in a single pulse with dosimetric properties suitable for small-animal experiments. We observed FLASH normal tissue sparing of radiation toxicities in mouse skin irradiated at 35 Gy with no sacrifice to tumor growth suppression. This study highlights an accessible new modality for laboratory study of the FLASH effect.

Corresponding author: Mohammad Rezaee, PhD; E-mail: mrezaee1@jh.edu

This work was supported by the National Cancer Institute (1R01CA262097-01) and the American Society for Radiation Oncology −American Association of Physicists in Medicine Trainee in Physics Research Award.

Disclosures: All authors report no conflicts of interest relevant to the submitted work.

All data are available upon request to the corresponding author.

Acknowledgments—The authors acknowledge Clifford Hammer and the University of Wisconsin Medical Radiation Research Center for their support in dosimeter calibration.

Int J Radiation Oncol Biol Phys, Vol. 117, No. 4, pp. 1018−1027, 2023
0360-3016/$ - see front matter © 2023 Elsevier Inc. All rights reserved.
https://doi.org/10.1016/j.ijrobp.2023.06.006

Introduction

Recent efforts have explored the remarkable widening of the therapeutic ratio from ultrahigh-dose-rate radiation (>37 Gy/s; FLASH) in comparison to conventional (CONV) dose-rate radiation (~0.1 Gy/s).[1] Through numerous preclinical studies, "FLASH effects," the reduced normal tissue injury and comparable tumor control incurred by treatment with FLASH radiation, have been demonstrated at doses >7 Gy in murine models across a wide variety of treatment sites such as brain,[2] lung,[3] abdomen,[4] and skin.[5] Investigation toward the translation of FLASH radiation therapy has already expanded into larger animal models[6] and is rapidly progressing toward application in human patients. The first human patient was treated with FLASH electrons in 2019,[7] and early results from the first-in-human clinical trial of FLASH proton radiation therapy (FAST-01) have been recently reported.[8,9] Despite the excitement and rapid development of technology to support clinical translation, the underlying mechanism and potential risks of FLASH radiation remain unclear. Severe late toxicities were observed in a veterinary clinical trial of nasopharyngeal tumor control in felines, resulting in discontinuation of the trial.[10,11] The National Cancer Institute has urged caution and thorough preclinical studies to support the translation of FLASH radiotherapy.[12] Intensive preclinical studies are still essential for clinical translation of FLASH radiation therapy to address several important challenges such as differential sensitivity of normal and tumor tissues to FLASH irradiation, dosimetric constraints for target (eg, PTV) and nontarget regions, and implications for spatial and temporal fractionation.

The existing state of FLASH radiation therapy research predominantly relies on high-energy electrons or protons generated by accelerators for medical or high-energy radiation research applications that are presently capable of producing appropriate ultrahigh dose rates.[13-16] However, these systems are complex and expensive, limiting their accessibility and utility for FLASH research to the majority of basic laboratory researchers. The complexity of available FLASH-capable equipment has resulted in highly variable dose rates and underlying pulse structures in the current body of preclinical research. As a result, no clear consensus exists on the requisite irradiation conditions (dose, instantaneous/average dose rate, maximum irradiation time, etc) to induce FLASH effects.

Kilovoltage x-ray sources have been proposed as a potential laboratory FLASH irradiator due to their low cost and wide commercial availability. Bazalova-Carter and Esplen have measured dose rates in excess of 100 Gy/s from a stationary anode x-ray source operating at 160 kVp and 6 kW input power without any energy filtration.[17] However, slow ramp-up times necessitated the use of a mechanical shutter, and the dose rates fell beneath 40 Gy/s beyond the initial 2 mm depth in phantoms. Rezaee et al proposed an alternative approach using rotating-anode x-ray sources with high input power (100 kW) and heat loading capacity, such as those currently used for fluoroscopic applications.[18] In a computational study using Monte-Carlo simulation platform, the authors demonstrated that an opposing pair of rotating-anode x-ray sources with 0.025-mm copper filtration can deliver dose rates >120 Gy/s with high-depth uniformity within a 2-cm-thick water phantom. A dosimetric evaluation of a 75-kW single-tube rotating-anode x-ray system was performed by Miles et al, demonstrating dose rates >90 Gy/s were achievable with adequate beam qualities for superficial targets in small-animal applications.[19]

In this work, we present the initial application of a single-source prototype of a high-capacity rotating-anode x-ray system for preclinical FLASH radiation study. This work demonstrates the first applications of orthovoltage x-rays from a commercially available x-ray tube for in vivo laboratory FLASH research.

Materials and Methods

FLASH x-ray irradiator

A high-capacity RAD44 x-ray tube (Varex Imaging, Salt Lake City, UT), supplied by a CPI Indico 100 RAD 80-kW generator (CPI Industries, Palo Alto, CA), was implemented as our exploratory FLASH x-ray irradiator (Fig. 1A). The tube and generator are operated using a CPI Indico Plus generator console (CPI Industries). This system and its dosimetric characteristics have been described in detail elsewhere.[19] Briefly, the x-ray tube features an inherent 0.7 mm of aluminum filtration with an additional 0.025-mm copper filter to ensure removal of electron contaminants from the tube and significant attenuation of low-energy photons (<25 keV). No wedge filter was used to compensate for anode heel effects to prevent additional beam attenuation and degradation of dose rate. The RAD44 tube features a conical opening (hereafter referred to as the flange of the x-ray tube) allowing samples to be placed close to the exit window, as shown in Fig. 1B. The distance between the focal spot and the exit window is 37.2 mm.

At the maximum operating voltage of 150 kV, the x-ray tube can receive a maximum input current of 500 mA and deliver a single-pulse exposure up to 500 ms. At these input parameters, a sample positioned 10 mm distal to the exit window (47 mm source-to-surface distance [SSD]) can be irradiated at a maximum dose rate of 96 Gy/s. The delivered dose and dose rate can be determined by adjusting the input current and exposure time, as well as the SSD. However, selection of the input parameters is limited in the control console by the tube load ratings in radiographic mode. Due to the mechanism of x-ray production with rotating-anode technology in its radiographic mode, all exposures consist of 1 continuous pulse at an average dose rate.

Irradiation setup and dosimetry

An in vivo experiment was devised to demonstrate the capability of the FLASH x-ray system to attain normal tissue

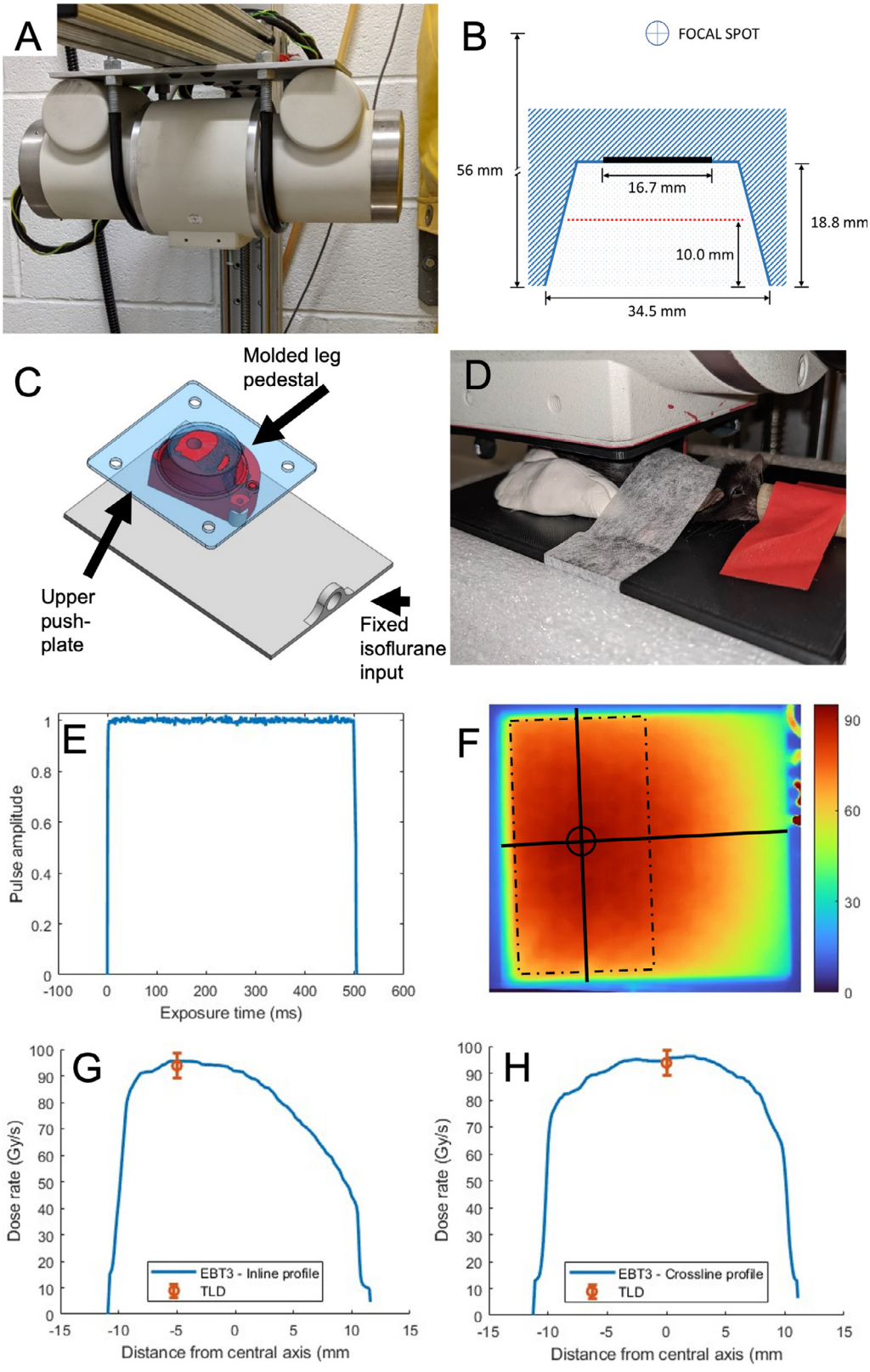

Fig. 1. Experimental setup and dosimetry of rotating-anode x-ray system for ultrahigh-dose-rate (>37 Gy/s; FLASH) irradiation of mouse skin model. (A) RAD44 x-ray tube used in this study for FLASH irradiation of mouse skin. (B) Conical opening (ie, the flange) of this tube that allows positioning of samples close to the exit window of the tube. (C) Custom 3-dimensionally printed immobilization tool to elevate a hind leg into the flange for FLASH irradiation. (D) Complete mouse setup for FLASH irradiation. (E) Pulse structure of a 500-ms FLASH exposure indicating consistent pulse amplitude, very rapid pulse ramp-up and ramp-down times, and accurate exposure timer. (F) Dose rate distribution (Gy/s) measured by EBT3 films at the surface

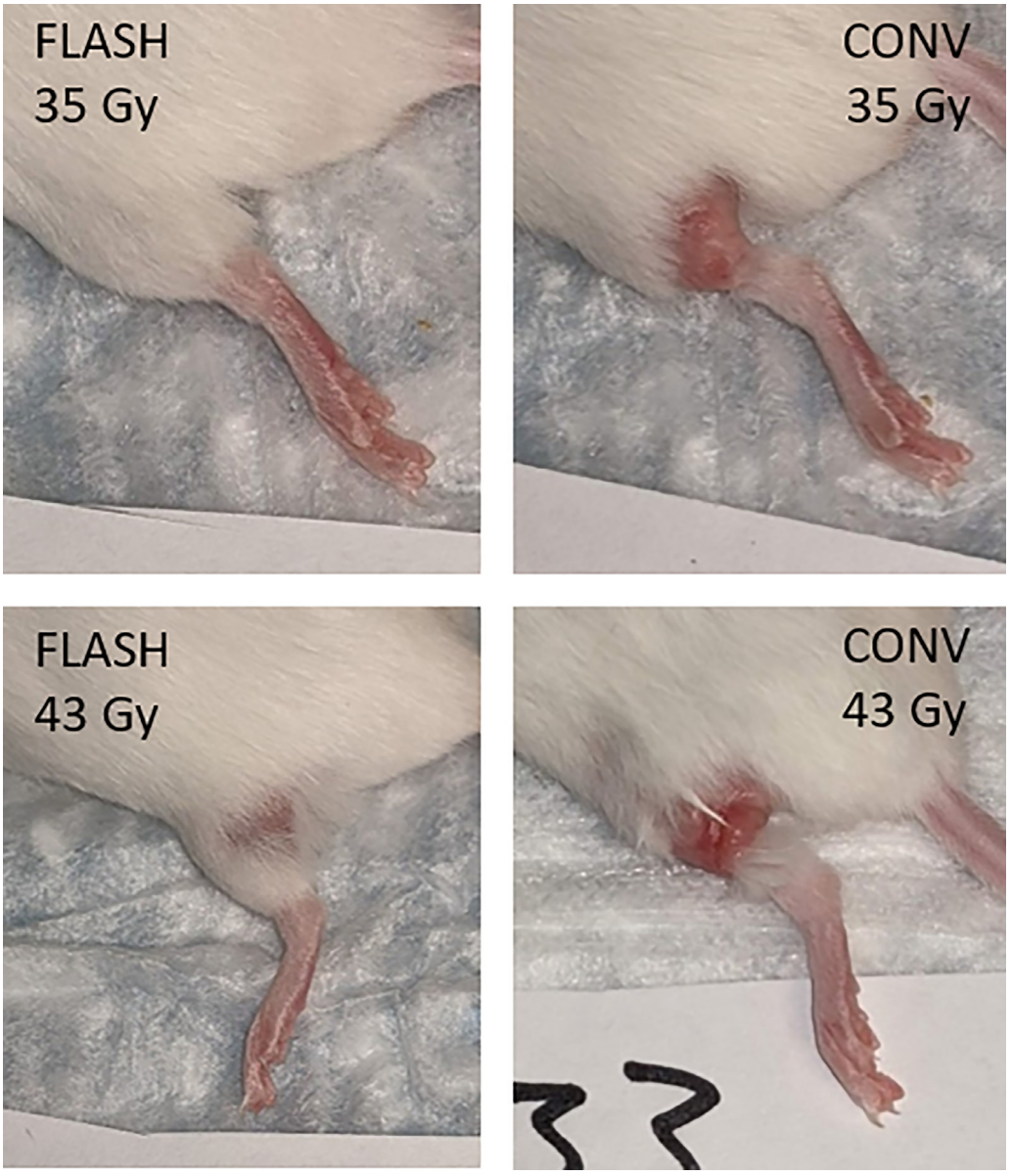

Fig. 2. Representative radiation skin toxicities induced by ultrahigh-dose-rate radiation (>37 Gy/s; FLASH) or conventional (CONV) x-ray radiation at 4 weeks postirradiation. CONV x-ray exposure resulted in more severe damage to the skin at both dose levels.

sparing effects on FLASH-irradiated skin in healthy mouse legs. This study was performed as per an Institutional Animal Care and Use Committee-approved protocol using inbred FVBN and FVBN/C57BL/6 outbred adult mice. Mice were irradiated on 1 hind leg using either FLASH x-rays at the highest achievable dose rate or using a small animal radiotherapy research platform (Xstrahl Inc, Suwanee, GA) at a CONV dose rate of 3 Gy/min. Table 1 summarizes the physical parameters used for both FLASH and CONV dose-rate irradiations. In both irradiators, a single top-down beam was used with the animal in the prone position. To achieve the highest dose rate possible on the FLASH irradiator, the mouse leg was elevated 10 mm inside the tube flange to an SSD of 47 mm using a custom 3-dimensionally printed immobilization tool as shown in Fig. 1C and 1D. A 3-dimensionally printed, 1-mm-thick polylactic acid plastic push-plate was rigidly fixed to the x-ray tube to ensure reproducible SSD and limit the leg's elevation into the flange for each mouse subject. The hind leg area positioned in the irradiation fields was 10 mm in the superior-inferior

of mouse leg in the FLASH irradiation setup. The mouse leg is positioned in the high-intensity region of the field (dashed box), with an average dose rate of 87 Gy/s. (G) Inline dose-rate profile showing anode-heel effects and (H) crossline dose-rate profile, both from EBT3 film measurement. Secondary TLD measurements in the high-intensity region of the field agree with EBT3 measurements to within 3%.

Table 1 Summary of physical parameters used for FLASH and CONV irradiation of murine skin

Irradiation parameter	FLASH	CONV
Peak energy of x-ray beam, kVp	150	220
Mean energy of x-ray beam, keV	52.5	63.0
Tube current, mA	500	13
Focal spot to mouse skin distance (SSD), mm	47	350
Number of x-ray pulses	1	1
Pulse width irradiation time, s	0.40, 0.50	700.0, 860.0
Dose levels, Gy	34.7 ± 1.6, 43.3 ± 2.0	35.0 ± 1.0, 45.0 ± 1.3
Average dose rate, Gy/s	86.7 ± 3.9	0.05
Instantaneous dose rates	NA	NA
Field size, mm	10 × 20	10 × 10
Focal spot size, mm	2.0	5.5
External energy filter, mm Cu	0.025	0.16

Abbreviations: CONV = conventional; FLASH = ultrahigh dose rate (>37 Gy/s); NA = not available; SSD = source-to-surface distance.

direction and <7 mm in the lateral direction. For CONV dose-rate irradiations on the small animal radiotherapy research platform, the largest fixed collimator (ie, 10 × 10 mm^2) was used to irradiate the mouse skin at 350 mm SSD. CONV irradiations used our institution's standard operating parameters of 220 kVp and 13 mA. For FLASH dose-rate irradiation, the field size was 10 × 20 mm^2, which covered 10 mm in the superior-inferior direction and 20 mm in the lateral direction. Because the target area extended <7 mm laterally, the difference in field dimension between CONV and FLASH dose-rate beams was expected to be negligible.

Dosimetric measurements to support in vivo study were performed using calibrated TLD and Gafchromic EBT3 film, which have both been previously demonstrated low dose-rate dependencies up to 10^6 Gy/s.[20-22] Both dosimeters were calibrated using a NIST-traceable, moderately filtered 120 kVp x-ray source (2.3 mm Al and 0.1 mm Cu), implemented by the University of Wisconsin Medical Radiation Research Center (UWMRRC).[23] This calibration source had beam quality similar to the RAD-44 x-ray tube used for this FLASH study.[18] A detailed description of the calibration x-ray source can be found elsewhere.[24]

For EBT3 film calibration, small cuts of film were shipped to UWMRRC for irradiation at known doses up to 10 Gy. Film was returned via 2-day shipping and immediately digitized using an Epson 11000XL flatbed scanner, operating at 300 dpi. The red-channel images were used to generate an optical-density-to-dose calibration curve using an in-house MATLAB script (The MathWorks, Inc), which was applied to all film exposures in this study. For in vivo dose measurements, a mouse carcass was positioned and irradiated in the setup tool used for our radiation skin toxicity study (Fig. 1D), with a cut of EBT3 film placed on top of the mouse's leg. The exposed film was digitized 24 hours after irradiation, and the calibration was applied to determine the delivered dose. Differences in optical density are expected to be <0.5% between 24 and 48 hours after exposure.[25] Beam flatness, symmetry, and dose uniformity were calculated, and beam output was compared with the point-dose TLD measurement. The uncertainty in this measurement is estimated to be 3.6% at the 95% confidence interval.

Secondary TLD measurements were conducted remotely through the UWMRRC. Briefly, TLD-100 microcubes (TLD-100; LiF:Mg,Ti; 1 × 1 × 1 mm^3) were sent to our laboratory from UWMRRC. A solid water phantom was manufactured with wells for loading TLDs, with 1.5-mm diameter and 1-mm deep cavities, to allow TLDs to be reproducibly positioned in-phantom. For this study, the TLD was positioned at the same SSD (47 mm) and location in the x-ray beam used for mouse irradiation. Buildup material of 1 mm was applied to mimic the buildup material used during mouse irradiation, with 15 mm of solid water distal to the TLD to ensure adequate backscattering conditions. After exposure, TLDs were returned to UWMRRC for readout. The uncertainty in this measurement is estimated at 5% at the 95% confidence interval.

For both dosimeters, the dose rate was determined based on the measured dose within the dynamic range of each detector and the requested exposure time from the x-ray generator. Output of the FLASH x-ray system has linear relationship with the tube exposure time.[19,26] This linearity was confirmed using EBT3 film measurement within its dynamic range, and it is used to calculate irradiation time required for the delivery of requested doses in this study. higher than According to the report number 99 from National Council of Radiation Protection and Measurement (NCRP99), the exposure timer accuracy for 3-phase x-ray generators used for medical applications must be accurate to within 5% for exposure durations above the minimum setting.[27] Accuracy of the exposure times from the RAD44 x-ray source used in this study was measured and confirmed using a RaySafe X2 with R/F sensor (Unfors Raysafe Inc, Glenwood, IL). In prior measurements, the ramp-up times for this system were submillisecond, thus not expected to contribute appreciable uncertainty in this measurement.[19] Using pulse form measured by RaySafe 2 detector in this study (Fig. 1E), the ramp-up times were <1 ms, which agrees with the previous measurement.

Radiation skin injury study

Doses of 35 Gy or 43 Gy, prescribed to the skin surface, were delivered in a single pulse of 150 kV x-rays to the hind flank of each mouse at the highest achievable FLASH dose rate (87 Gy/s), using the maximum current setting on our FLASH generator control console (500 mA) at exposure durations of 400 ms and 500 ms, respectively. The FLASH

doses were determined based on the EBT3 film measurements in the previous section. In a parallel arm of this study, CONV dose rate (3 Gy/min) radiation was delivered to mice at the same dose levels. These doses were chosen to match those used in prior FLASH proton and electron experiments that have demonstrated skin sparing effects at comparable dose rates.[28,29] A minimum of 6 mice were irradiated at each dose level per dose rate (n = 6-7 per experimental condition), with the strains distributed as evenly as possible across the experimental arms. A summary of the mice used per each irradiation condition is indicated in Table 2. Animal cages were changed weekly to limit the risk of bacterial infection and potential irritation to the irradiated skin. Mice that developed severe skin injury noted by our veterinary staff were treated with a single dose of Buprenorphine SR and daily topical application of Neosporin.

At 8 weeks postirradiation, all mice were assessed for presence of radiation-induced ulceration and skin sections were harvested for histopathologic assessment with endpoints of fibrosis, epidermis hyperplasia, and inflammation. Tissue sections were fixed in 10% buffered formalin and processed using the standard hematoxylin and eosin and

Table 2 Overview and results of radiation-induced skin injury experiments

				8 wk postirradiation			
Radiation condition	Strain	Sex	Age at IR (wk)	Ulceration visibility	Epidermis thickness (μm)	Dermis cell density (per area)	Collagen density (% area)
CONV 35 Gy	FVBN	F	8	N	67	0.138	0.972
	FVBN	M	8	N	171	0.115	0.955
	FVBN	M	9	Y	252	0.117	0.828
	FVBN	M	9	Y	247	0.197	0.872
	FVBN	F	13	Y	569	0.086	0.657
	C57BL6	F	14	Y	174	0.125	0.704
CONV 43 Gy	FVBN	M	9	Y	149	0.165	0.954
	FVBN	M	9	Y	158	0.136	0.905
	FVBN	F	12	Y	276	0.095	0.905
	C57BL6	F	13	N	105	0.095	0.731
	C57BL6	F	14	Y	458	0.128	0.890
	C57BL6	F	14	Y	75	0.077	0.722
FLASH 35 Gy	FVBN	M	8	N	23	0.022	0.753
	FVBN	F	9	N	73	0.137	0.888
	C57BL6	F	14	N	46	0.076	0.737
	C57BL6	F	14	N	169	0.122	0.606
	C57BL6	F	14	N	16	0.065	0.697
	FVBN	F	16	N	27	0.047	0.625
FLASH 43 Gy	FVBN	F	9	Y	266	0.141	0.816
	FVBN	M	12	N	82	0.052	0.668
	C57BL6	F	13	N	184	0.141	0.905
	C57BL6	F	13	N	218	0.122	0.934
	C57BL6	F	14	N	113	0.137	0.940
	FVBN	F	16	N	324	0.124	0.925
Untreated	FVBN	F	8	N	14	0.074	0.643
	C57BL6	F	8	N	14	0.052	0.572
	FVBN	F	9	N	16	0.052	0.655
	FVBN	M	9	N	23	0.024	0.624

Readily available mice of varying strains, sexes, and ages were divided evenly throughout this experiment.
Abbreviations: CONV = conventional; F = female; FLASH = ultrahigh dose rate (>37 Gy/s); IR = irradiation; M = male.

Masson's trichrome staining procedures at our institution's oncology tissue services core. Whole slides were digitized for analysis using a NanoZoomer slide scanner (Hamamatsu Photonics, Japan). Analysis was performed with support of a comparative pathologist for endpoints of fibrosis, inflammation, and epidermal hyperplasia. Hyperplasia was determined based on changes of the measured thickness of the epidermis compared with baseline. Inflammation was quantified based on the number of hematoxylin-stained nuclei per area in the dermis relative to the unirradiated control samples. Fibrosis was determined based on the density of blue-stained collagen from trichrome stain. All histology quantification was performed using ImageJ[30] and statistical significance was calculated using a 2-tailed Student *t* test.

Tumor growth delay assessment

Tumor growth delay after FLASH kV x-rays was assessed using a flank melanoma tumor model in 8-week C57BL6 mice. B16F10 cells were cultured in high-glucose Dulbecco's Modified Eagle Medium (#11965092, Gibco) supplemented with 10% fetal bovine serum (#35-011-CV, Corning). Cells were trypsinized when 80% confluency was reached. Trypsinized cells were washed and resuspended in an ice-cold medium of 50% Matrigel (#CLS354234, Corning) and sterile phosphate buffered saline at a density of 1.5×10^6 per mL. C57BL6J mice were then inoculated in the hind flank with 1.5×10^5 cells and tumors were allowed to propagate until the basal diameter exceeded 5 mm, approximately at 1.5 weeks. The tumor size was chosen to restrict the thickness of tumor tissue and limit the potential confounding factor of the depth-dose gradient on this experiment.

Flank tumors were positioned at the same region of the x-ray beam used for the normal tissue injury experiment on the mouse leg, described in the previous section. Tumors were irradiated to 35 Gy at FLASH or CONV dose rates with a circular field of 10 mm in diameter. Each experimental arm included 5 mice, per each dose rate and unirradiated samples. After irradiation, tumor volume was tracked twice per week with digital calipers. Volume was calculated as $(L \times W \times H \times \pi/6)$. Statistical significance was calculated using a paired Student *t* test.

Results

X-ray FLASH surface dosimetry

FLASH beam was delivered in the radiographic mode of the x-ray source using a single continuous pulse with less than 0.5 ms uncertainty in the exposure time and desired pulse consistency (ie, 0.7% variations in the pulse amplitude; Fig. 1E). These inaccuracies in exposure time and pulse consistency produce negligible dosimetric error in this study. Figure 1F to 1H shows a summary of in vivo and phantom dosimetry results. The maximum dose rate measured by EBT3 films was 91.3 ± 3.3 Gy/s, which occurred near the cathode-side of the radiation beam. The TLD point-dose measurement was acquired at the same location, with a comparable dose rate of 93.8 ± 4.9 Gy/s. Film and TLD dosimetry measurements agreed to within 3%. The average dose rate in the usable 10 × 20 mm field on the cathode-half of the beam was 86.7 ± 3.9 Gy/s, which was measured with EBT3 film. The achievable mean doses to the leg surface using the field were 34.7 ± 1.6 and 43.3 ± 2.0 Gy for the exposure times of 400 and 500 ms at the tube current of 500 mA, respectively. These dose levels are rounded to 35 and 43 Gy for reference throughout this article. The flatness and symmetry of the 10 × 20 mm field were ±3.3% and ±4.7%, respectively. These dosimetric results were adequate to study FLASH effects on superficial targets such as murine skin model.

X-ray FLASH skin toxicity

Injuries to the irradiated skin were visible as early as 4 weeks postirradiation, as shown in Fig. 2. At both dose levels, FLASH-treated mice experienced partial or complete alopecia (hair loss) in the irradiated area but did not typically progress to more severe skin toxicities. Only 1 FLASH-irradiated mouse at 43 Gy experienced ulceration. More severe skin injury was commonly observed in conventionally treated mice, with ulceration occurring in 57% and 71% of mice irradiated at 35 Gy and 43 Gy CONV x-rays, respectively.

Histopathologic assessment at 8 weeks postirradiation confirms the potential radioprotective effects of FLASH x-rays at the dose level of 35 Gy, as shown in Figure 3 and Table 2. At 35 Gy, FLASH-irradiated samples significantly differ from the CONV-irradiated samples with respect to the endpoints of skin hyperplasia and inflammation formation ($P < .01$). For the same samples, differences in radiation-induced fibrosis between FLASH and CONV irradiated samples were marginally statistically significant ($P = .057$). In addition, the samples received 35 Gy from FLASH x-rays did not show significant difference from untreated control samples with respect to hyperplasia, inflammation, or fibrosis at 8-week after irradiation ($P > .1$). There was not a significant difference between FLASH and CONV irradiated samples at 43 Gy for the less-severe endpoints used for histopathologic assessment. The samples irradiated by FLASH 43 Gy, CONV 35 Gy, and CONV 43 Gy were significantly different from baseline for hyperplasia, fibrosis, and inflammation ($P < .05$).

X-ray FLASH tumor growth delay

Tumor growth was suppressed at both FLASH and CONV dose rates after a 35-Gy exposure. This dose level was selected because of persistent observation of FLASH effects on the sparing of healthy mice skin in the histopathologic assessment explained in the previous section. Figure 4 shows

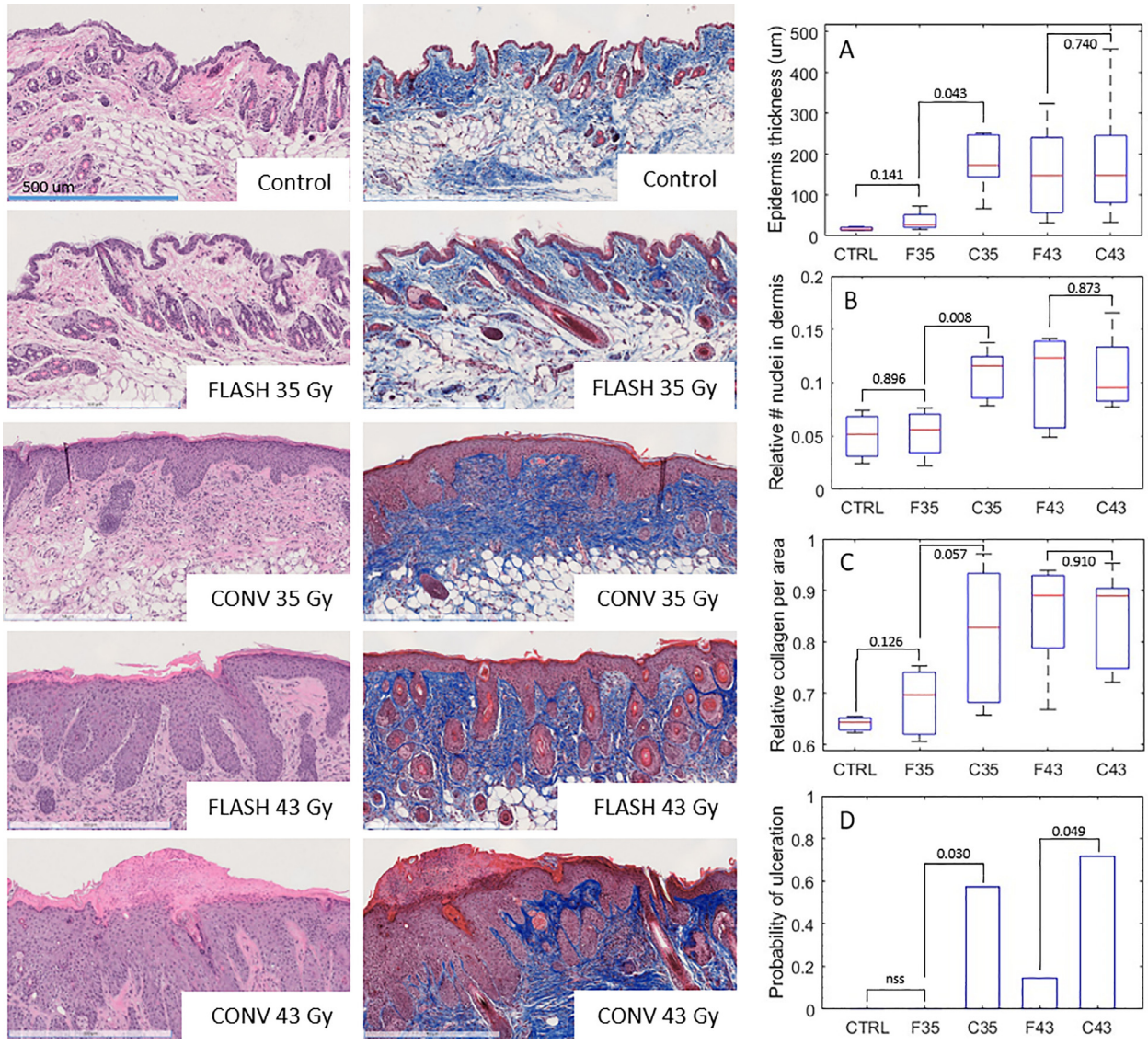

Fig. 3. Pathologic assessment of skin toxicities after ultrahigh-dose-rate radiation (>37 Gy/s; FLASH) and conventional (CONV) x-ray radiation. Representative tissue sections stained with hematoxylin and eosin (left column) and Masson's trichrome (middle column). Comparison between treatment groups for endpoints of hyperplasia (A), inflammation (B), fibrosis (C), and ulceration (D) reveal a significant sparing of normal tissue injury from 35 Gy of FLASH radiation. FLASH normal tissue sparing at higher doses is observed only for higher-severity endpoints (ulceration).

a decrease in the tumor volume for all irradiated samples within 2 weeks after irradiation, whereas unirradiated tumors grew exponentially. No statistically significant difference was observed in tumor growth between FLASH and CONV dose rates for all assessed timepoints ($P > .2$). Tumor volume tracking ended at 2 weeks post irradiation due to the difficulty of identifying a palpable tumor mass. Control mice were euthanized when the largest tumor dimension exceeded 15 mm.

Discussion

The rotating-anode x-ray tube used in this study was capable of producing kV x-rays at dose rates well above 40 Gy/s at short SSD. Delivery of doses up to 43 Gy at ultrahigh dose rates (87 Gy/s) to superficial targets were feasible for murine skin irradiation. The inherent anode heel effect resulted in a gradient in dose output and dose rates along the heel axis of the beam. Although our results show that the intensity of the beam was sufficiently uniform in our predefined field location for our feasibility studies, appreciable dosimetry uncertainties can result from sample positioning errors outside of this region. Dosimetric uncertainties from ramp-up time and exposure timer were negligible, even shorter than 1 ms. Contribution of electrons and low-energy x-rays in the beam were also negligible due to using an external Cu filter. These features altogether allow us to overcome many limitations of stationary-anode technology[17] to use orthovoltage x-rays for preclinical FLASH radiation therapy research.

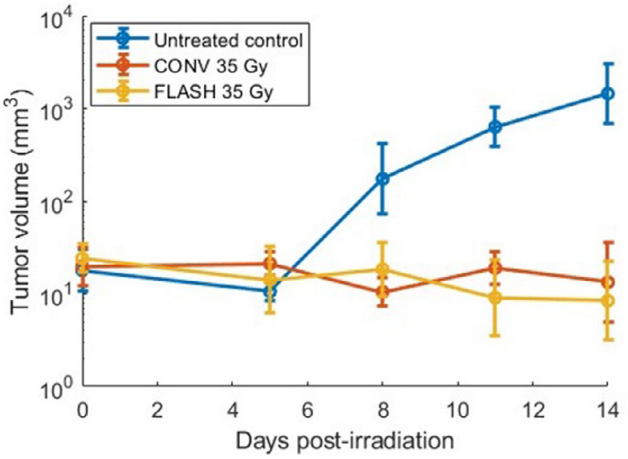

Fig. 4. Tumor volume as a function of time for 14 days after ultrahigh-dose-rate (>37 Gy/s; FLASH) and conventional (CONV) irradiations. No difference in tumor growth was observed after a single fraction of 35 Gy at FLASH or CONV dose rates. Tumor volumes were tracked until a mass could no longer be palpated.

Significant normal tissue sparing effects, without sacrifice to tumor kill, were observed after the delivery of 35 Gy in 400 ms at the dose rate of 87 Gy/s in a mouse skin and melanoma flank tumor model. Normal tissue sparing effects were visible in the affected leg and quantified using endpoints of ulceration, hyperplasia, inflammation, and fibrosis. The results of our initial skin injury experiment were in agreement with those performed using high-energy protons[5,29,31] and electrons[27] at FLASH dose rates, confirming that orthovoltage x-rays are capable of inducing FLASH effects. To compare with prior works, Soto et al[28] demonstrated a significant difference in skin scoring between FLASH and CONV dose rate electrons at 40 Gy, with a similar significance between experiment arms that reached their euthanasia criteria at both 30 and 40 Gy. Velalopoulou et al[5] assessed skin toxicity scoring after proton irradiation at FLASH or CONV dose rates and reported a similar sparing of skin toxicity seen in our current work with respect to hyperplasia at doses of 30 Gy and ulceration at doses of 45 Gy. Singers et al[31] reported dose response curves to induce varying severities of radiation-induced skin injury with FLASH and CONV dose-rate protons, showing the probability of inducing low-severity injuries exceeding 50% from doses of 25 Gy at CONV dose rates and 39 Gy at FLASH dose rates. Reported high-severity injuries occur in 50% of animals at doses >47 Gy at FLASH dose rates or 32 Gy at CONV dose rates. These results agree with our observation that FLASH normal tissue sparing effects for lower-severity histopathologic endpoints of hyperplasia, inflammation, and fibrosis disappear at 43 Gy, while apparent difference in high-severity endpoint of ulceration is still observable between FLASH and CONV irradiation. Velalopoulou et al and Singers et al both demonstrated no loss of tumor control from ultrahigh-dose proton therapy in subcutaneous sarcoma and mammary carcinoma tumor models, respectively, after single-fraction doses ranging from 12 to 60 Gy.

In contrast with prior FLASH proton and electron skin toxicity experiments, this work differs in 2 notable ways. The first is the variety of mouse strain. FVB/N are white-haired mice not used previously for FLASH studies to assess skin sparing. In addition, some of our mice were a mixed breed FVB/N and C57BL/6J background more like those reported in previous FLASH effect studies. The second deviation is the pulse structure of the kV x-ray beam. Although the aforementioned murine skin toxicity studies used high-frequency pulses of electrons and protons, the system described in this work produces x-rays in a single, high-dose, continuous pulse. The importance of pulse structure, dose per pulse, and pulse rates to induce FLASH effects remains under wide scrutiny,[32] with no current consensus on ideal parameters. Although our results are preliminary, it could be inferred that the average dose rate per delivery is the critical parameter to induce FLASH effects, not necessarily the underlying pulse structure of the beam.

Further developments to rotating-anode x-ray tube technology include the prototyping of a self-shielded cabinet-style irradiator for x-ray FLASH research. A design for such a system has been described by Rezaee et al.[18] This design would overcome major dosimetric shortcomings of the single-source rotating-anode irradiator, including sharp dose falloff with depth and heterogeneous in-line profile, through implementation of 2 opposing orthovoltage x-ray sources with opposing heels. Monte Carlo modeling of this dual-source system demonstrates a highly uniform dose deposition for samples up to 20 mm thick, with field sizes on the order of 20×20 mm^2 and dose rates >120 Gy/s. The development of a dual-source system for orthovoltage x-ray FLASH research remains in progress.

Conclusion

This work demonstrates compelling evidence supporting the capacity of rotating-anode x-ray sources to induce FLASH effects through an in vivo skin toxicity and tumor growth delay study. The irradiator used in this study is capable of producing a single pulse of FLASH x-rays at dose rates up to 94 Gy/s, with a field size adequate for small-animal irradiation studies. This work is expected to lay the foundation for a new direction of FLASH research using economical, laboratory-accessible irradiation platforms.

References

1. Favaudon V, Caplier L, Monceau V, et al. Ultrahigh dose-rate FLASH irradiation increases the differential response between normal and tumor tissue in mice. *Sci Transl Med* 2014;6 245ra93.
2. Simmons DA, Lartey FM, Schüler E, et al. Reduced cognitive deficits after FLASH irradiation of whole mouse brain are associated with less hippocampal dendritic spine loss and neuroinflammation. *Radiother Oncol* 2019;139:4-10.

3. Fouillade C, Curras-Alonso S, Giuranno L, et al. FLASH irradiation spares lung progenitor cells and limits the incidence of radio-induced senescence. *Clin Cancer Res* 2020;26:1497-1506.
4. Levy K, Natarajan S, Wang J, et al. Abdominal FLASH irradiation reduces radiation-induced gastrointestinal toxicity for the treatment of ovarian cancer in mice. *Sci Rep* 2020;10:21600.
5. Velalopoulou A, Karagounis IV, Cramer GM, et al. FLASH proton radiotherapy spares normal epithelial and mesenchymal tissues while preserving sarcoma response. *Cancer Res* 2021;81:4808-4821.
6. Vozenin MC, De Fornel P, Petersson K, et al. The advantage of FLASH radiotherapy confirmed in mini-pig and cat-cancer patients. *Clin Cancer Res* 2019;25:35-42.
7. Bourhis J, Sozzi WJ, Jorge PG, et al. Treatment of a first patient with FLASH-radiotherapy. *Radiother Oncol* 2019;139:18-22.
8. Mascia AE, Daugherty EC, Zhang Y, et al. Proton FLASH radiotherapy for the treatment of symptomatic bone metastases: The FAST-01 nonrandomized trial. *JAMA Oncol* 2023;9:62-69.
9. Daugherty EC, Mascia A, Zhang Y, et al. FLASH Radiotherapy for the Treatment of Symptomatic Bone Metastases (FAST-01): Protocol for the first prospective feasibility study. *JMIR Res Protoc* 2023;12:e41812.
10. Rohrer Bley C, Wolf F, Gonçalves Jorge P, et al. Dose- and volume-limiting late toxicity of FLASH radiotherapy in cats with squamous cell carcinoma of the nasal planum and in mini pigs. *Clin Cancer Res* 2022;28:3814-3823.
11. Maity A, Koumenis C. Shining a FLASHlight on ultrahigh dose-rate radiation and possible late toxicity. *Clin Cancer Res* 2022;28:3636-3638.
12. Buchsbaum JC, Coleman CN, Espey MG, et al. FLASH radiation therapy: New technology plus biology required. *Int J Radiat Oncol* 2021;110:1248-1249.
13. Lin B, Gao F, Yang Y, et al. FLASH radiotherapy: History and future. *Front Oncol* 2021;11:644400.
14. Schüler E, Trovati S, King G, et al. Experimental platform for ultra-high dose rate FLASH irradiation of small animals using a clinical linear accelerator. *Int J Radiat Oncol* 2017;97:195-203.
15. Diffenderfer ES, Verginadis II, Kim MM, et al. Design, implementation, and in vivo validation of a novel proton FLASH radiation therapy system. *Int J Radiat Oncol* 2020;106:440-448.
16. Patriarca A, Fouillade C, Auger M, et al. Experimental set-up for FLASH proton irradiation of small animals using a clinical system. *Int J Radiat Oncol* 2018;102:619-626.
17. Bazalova-Carter M, Esplen N. On the capabilities of conventional x-ray tubes to deliver ultra-high (FLASH) dose rates. *Med Phys* 2019;46:5690-5695.
18. Rezaee M, Iordachita I, Wong JW. Ultrahigh dose-rate (FLASH) x-ray irradiator for pre-clinical laboratory research. *Phys Med Biol* 2021;66 095006.
19. Miles D, Sforza D, Wong JW, et al. Dosimetric characterization of a rotating anode x-ray tube for FLASH radiotherapy research. *Med Phys* 2023;1-10. https://doi.org/10.1002/mp.16609.
20. Jaccard M, Petersson K, Buchillier T, et al. High dose-per-pulse electron beam dosimetry: Usability and dose-rate independence of EBT3 Gafchromic films. *Med Phys* 2017;44:725-735.
21. Jorge PG, Jaccard M, Petersson K, et al. Dosimetric and preparation procedures for irradiating biological models with pulsed electron beam at ultra-high dose-rate. *Radiother Oncol* 2019;139:34-39.
22. Karsch L, Beyreuther E, Burris-Mog T, et al. Dose rate dependence for different dosimeters and detectors: TLD, OSL, EBT films, and diamond detectors. *Med Phys* 2012;39:2447-2455.
23. Hammer CG, Rosen BS, Fagerstrom JM, Culberson WS, DeWerd LA. Experimental investigation of GafChromic® EBT3 intrinsic energy dependence with kilovoltage x rays, ^{137}Cs, and ^{60}Co. *Med Phys* 2018;45:448-459.
24. Moga JD. Characterization of low-energy photon-emitting brachytherapy sources and kilovoltage x-ray beams using spectrometry. Dissertation. University of Wisconsin − Madison; 2011. Available at: https://www.proquest.com/docview/929143173/abstract/441C3E2599CB4B2CPQ/1. Accessed May 9, 2022.
25. Borca VC, Pasquino M, Russo G, et al. Dosimetric characterization and use of GAFCHROMIC EBT3 film for IMRT dose verification. *J Appl Clin Med Phys* 2013;14:158-171.
26. Miles D, Sforza D, Wong JW, Rezaee M. Dosimetric study of a rotating anode x-ray tube for laboratory FLASH radiotherapy research. *Med Phys* 2022;49:E568.
27. National Council on Radiation Protection and Measurements. *Quality Assurance for Diagnostic Imaging Equipment: Recommendations of the National Council on Radiation Protection and Measurements*. Bethesda, Maryland: National Council on Radiation Protection and Measurements; 1988.
28. Soto LA, Casey KM, Wang J, et al. FLASH irradiation results in reduced severe skin toxicity compared to conventional-dose-rate irradiation. *Radiat Res* 2020;194:618-624.
29. Cunningham S, McCauley S, Vairamani K, et al. FLASH proton pencil beam scanning irradiation minimizes radiation-induced leg contracture and skin toxicity in mice. *Cancers* 2021;13:1012.
30. Schneider CA, Rasband WS, Eliceiri KW. NIH Image to ImageJ: 25 years of image analysis. *Nat Methods* 2012;9:671-675.
31. Singers SB, Krzysztof SM, Ankjærgaard C, et al. In vivo validation and tissue sparing factor for acute damage of pencil beam scanning proton FLASH. *Radiother Oncol* 2022;167:109-115.
32. Bourhis J, Montay-Gruel P, Gonçalves JP, et al. Clinical translation of FLASH radiotherapy: Why and how? *Radiother Oncol* 2019;139:11-17.